

In-plane thermoelectric power of c -axis-oriented $\text{Sr}_{1-x}\text{Nd}_x\text{CuO}_{2-\delta}$ thin films

Nobuyuki Sugii and H. Yamauchi

*Superconductivity Research Laboratory, International Superconductivity Technology Center,
10-13 Shinonome 1-chome, Koto-ku, Tokyo 135, Japan*

(Received 17 February 1994; revised manuscript received 6 June 1994)

We measured the in-plane thermoelectric-power coefficients (S) of c -axis-oriented $\text{Sr}_{1-x}\text{Nd}_x\text{CuO}_{2-\delta}$ ($0 \leq x \leq 0.125$) thin films deposited by means of a pulsed-laser deposition technique. The sign of S was negative for all the samples deposited on SrTiO_3 substrates and its absolute value decreased with increasing x . The value of S for $\text{Sr}_{1-x}\text{Nd}_x\text{CuO}_{2-\delta}$ with $x = 0.125$ was demonstrated to be strongly dependent on the substrate material on which the a -axis length depended. On the other hand, the value of S for $\text{Sr}_{1-x}\text{Nd}_x\text{CuO}_{2-\delta}$ with $x = 0.05$ was found to be rather weakly dependent on the a -axis length. These observations were discussed based on bond-valence-sum calculations. The variation in S of the $x = 0.125$ sample was attributed to the change in the electronic structure.

I. INTRODUCTION

Superconducting cuprates of the "infinite-layer" structure such as $(\text{Sr},\text{L})\text{CuO}_2$ ($\text{L} = \text{Nd}, \text{Pr}, \text{or La}$) were synthesized under high pressure and found to exhibit n -type superconductivity with transition temperatures (T_c 's) around 40 K.^{1,2} Since the infinite-layer structure is simple compared with the structures of any other known cuprate superconductors, infinite-layer cuprates would be useful for the study on the nature of high-temperature superconductivity. So far, such compounds have been synthesized only by high-pressure synthesis and vapor-deposition techniques, and no single crystals of the compounds have been obtained. Therefore, for the moment, to prepare high-quality thin-film samples is one of the best ways for the study on the nature of infinite-layer compounds.

There have been several reports on the fabrication of thin films of $(\text{Sr},\text{L})\text{CuO}_2$.³⁻⁵ In our previous work,⁶ we synthesized single-phase $\text{Sr}_{1-x}\text{Nd}_x\text{CuO}_{2-\delta}$ (SNCO) thin-film samples, and found that the superconducting property of the film was improved when fabricated on a Pr_2CuO_4 (PCO) "underlayer" grown on a SrTiO_3 (STO) substrate. This result suggested that the lattice matching between the film and the substrate is important for the fabrication of high-quality SNCO thin films. This is probably a consequence of the fact that the Cu-O bond length which is related to the a -axis length, i.e., the lattice length along the plane in the infinite-layer structure, is strongly dependent on the carrier concentration and electronic structure. For the SNCO films, the a -axis length indeed changed, as the a axis of the underlayer material changed.⁶ When a SNCO film was deposited on an underlayer material having the a axis shorter than that of the film material, the film would receive a compressive stress, and vice versa. It is known that, as electrons as charge carriers are doped into the CuO_2 planes, the Cu-O bond length should be elongated. Therefore, such stress in the lattice plane would hinder electron doping in and metallization of the SNCO films.

In this study, we measure thermoelectric-power coefficients in the ab plane of SNCO, and study the dependences on the Nd content and the lattice dimension in the ab plane. The change in S due to the lattice stress is discussed based on bond-valence-sum calculations.

II. EXPERIMENTS

The thin-film samples were prepared by a pulsed-laser deposition technique (PLD). An ArF excimer laser was used as the light source. The targets were prepared by a solid-state reaction method. SrTiO_3 (STO) single-crystal wafers with the (100) orientation was used as substrate materials. The substrate temperature was in the range 550–700°C. The distance between target and substrate was set at 100 mm. The deposition was performed in an oxygen gas of 0.13 Pa or a high-purity ozone gas of 0.013 Pa. The number of laser pulse shots to yield a film thickness of approximately 450 Å was 3×10^4 . After deposition, the film was kept in a vacuum for half an hour and cooled at a rate of 20°C/min. The background pressure was lower than 10^{-4} Pa. Several film samples were prepared on each of different kinds of underlayers of L_2CuO_4 ($\text{L} = \text{Pr}, \text{Nd}, \text{and Sm}$), all of which have a T' -type structure and formed on (100) STO substrate materials. The thickness of an underlayer was in the range 70–150 Å. The chemical composition of several samples were determined by inductively coupled plasma spectrometry and were confirmed to be stoichiometric within an experimental error of $\sim 5\%$.

The crystallographic properties of films were investigated by x-ray-diffraction analysis. Conventional θ - 2θ measurements were performed by a two-circle diffractometer using CuK_α radiation. The lattice constants were measured by a four-circle diffractometer using MoK_α radiation.

Thermoelectric-power coefficients for the samples were measured by a dc method. The temperature gradient (ΔT) in the sample was measured using two pairs of Cu-Constantan thermocouples. The thermocouples were at-

tached with Ag paste onto the Au electrodes sputter-deposited on the sample. The magnitude of ΔT was kept in the range 0.3–4 K during the measurement. To eliminate the effects from the reference leads (Cu wires), the absolute thermoelectric power of Cu was subtracted from the measured thermoelectric voltage. In general, for a thin-film sample, the as-measured value is not the intrinsic one because it contains contributions from both the underlayer and the substrate material. For a multiband system, S may be given by⁷

$$S = \sum_i \left[\frac{\sigma_i}{\sigma} \right] S_i, \quad (1)$$

where σ is the total conductivity, and σ_i and S_i are the conductivity and the thermoelectric-power coefficient for band i . Actually, the resistivities of the STO substrate and the underlayer material [$L_2\text{CuO}_4$ ($L=\text{Pr}$, Nd , and Sm)] were more than 2 orders of magnitude higher than those for SNCO films with the Nd contents higher than 0.05. Therefore, in the present samples, the contributions from the underlayer and the substrate material are considered to be negligibly small.

III. RESULTS

A. X-ray-diffraction analysis

All the samples with $x \leq 0.125$ were found to consist of single-phase infinite-layer compounds. The x-ray-diffraction pattern for a typical sample is shown in Fig. 1. The peaks indexed with $00l$ are those from the film. The peaks marked with “U” and “S” are those from the underlayer and the substrate material, respectively. No peaks due to impurity phases were observed. We often observed Laue functional intensity oscillations around the film peaks. This suggested that the surface smoothness and the crystallinity of the film were excellent, with the film thickness being as thin as 500 Å.

Figure 2 shows the variations in the lattice constants with the Nd content, x , for a film deposited on a bare

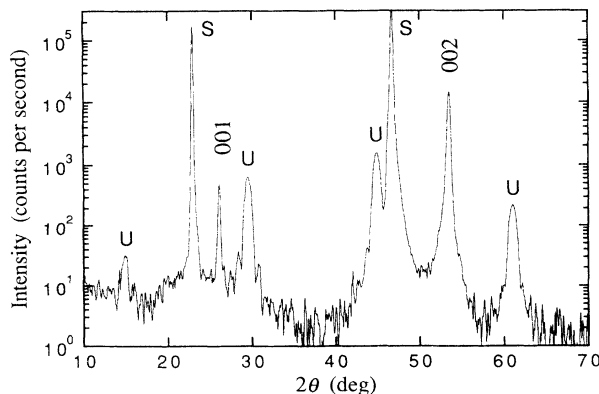


FIG. 1. X-ray-diffraction pattern for $\text{Sr}_{0.95}\text{Nd}_{0.05}\text{CuO}_{2-\delta}$ thin film with an Nd_2CuO_4 underlayer deposited on a (100) SrTiO_3 substrate. The peaks indexed with $00l$ are those from the film. The peaks marked with “U” and “S” are those from the underlayer and the substrate material, respectively.

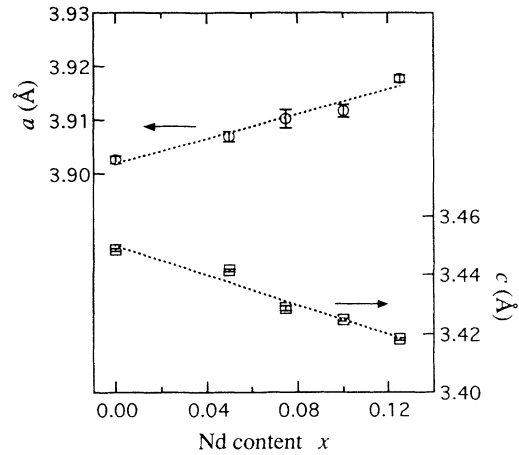


FIG. 2. The lattice constants for $\text{Sr}_{1-x}\text{Nd}_x\text{CuO}_{2-\delta}$ thin films as a function of Nd content, x . The films were deposited directly on SrTiO_3 substrates.

(100) STO substrate. With increasing x , the a -axis length became longer and the c -axis length shorter. The solubility limit was around $x = 0.125$. As we previously reported,⁴ the a -axis length was always shorter than those of the bulk samples prepared under high pressure.¹ When films were deposited on underlayers which were formed on STO, the a -axis length varied in correspondence with that of the underlayer material. It has been revealed that, the a axis of an underlayer material is close to that of the corresponding bulk material and the a -axis of a SNCO film is dependent on that of the underlayer, even when the thickness of the SNCO film is thicker than that of the underlayer. It suggests that the relaxation of the lattice mismatch between the SNCO film and the underlayer is less easy to occur than that between the underlayer material and STO.

B. Thermoelectric-power coefficients of the SNCO films with various Nd contents

The temperature dependences of thermoelectric-power coefficients (S) for the SNCO films deposited on bare STO substrates are shown in Fig. 3. The sign of S for all the samples was negative and the absolute value of S decreased as x increased, but saturated for $x \geq 0.10$. All the S -vs- T curves exhibit broad peaks and the values of S looks to approach to zero below few degrees (in K). The peak temperature decreased with increasing x . These behaviors observed for the SNCO films are similar to those observed for $\text{Nd}_2\text{CuO}_{4-x}\text{F}_x$ of the T' structure.⁸

In Fig. 4, the temperature dependence of electrical resistivity is shown for the SNCO films deposited on bare STO substrates. Near room temperature electrical resistivity decreased with increasing the Nd content. No samples exhibited metallic behavior. The samples with $x = 0.10$ and 0.125 exhibited superconductivity with the onset points in the resistivity-vs-temperature curves around 10 and 20 K, respectively. Nonetheless, zero-resistance states were not observed at temperatures above

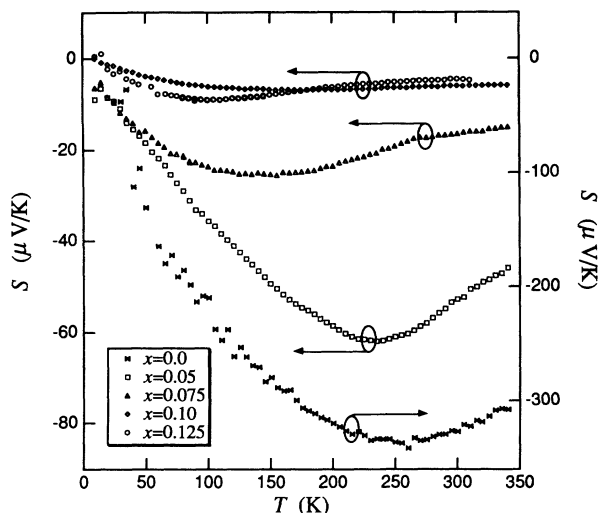


FIG. 3. Temperature dependence of thermoelectric-power coefficient (S) for the $\text{Sr}_{1-x}\text{Nd}_x\text{CuO}_{2-\delta}$ thin films with various Nd contents. The films were deposited directly on SrTiO_3 substrates.

4.2 K for both the samples. The resistivity data for the sample with $x=0.05$ showed an anomalous temperature dependence: resistivity decreased as the temperature decreased from 230 to 60 K. However, there were no anomalies in the temperature dependence of thermoelectric-power coefficient. We suppose that the anomaly in the resistivity-vs-temperature relation is due to the crossover of different temperature dependences of resistivity for the matrix and the grain boundaries or the defects. Similar anomalies have been reported by Norton *et al.*⁹ for reduced thin-film samples of infinite-layer $\text{Sr}_{1-x}\text{CuO}_{2-\delta}$.

C. Thermoelectric-power coefficients of the SNCO films formed on various underlayer materials

SNCO films with $x=0.125$ were deposited on a bare STO and two kinds of underlayer materials, Pr_2CuO_4

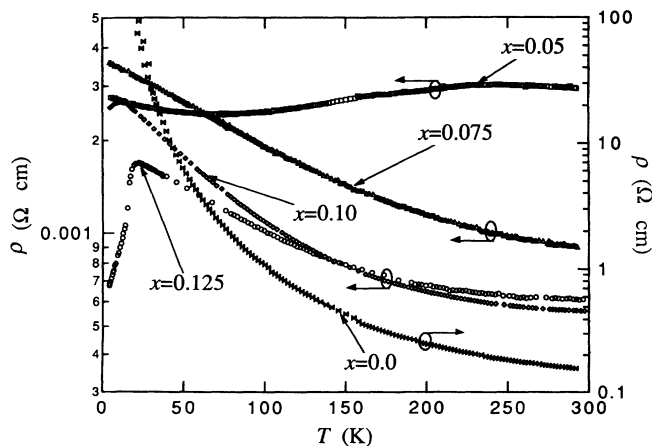


FIG. 4. Temperature dependence of resistivity for the $\text{Sr}_{1-x}\text{Nd}_x\text{CuO}_{2-\delta}$ thin films with various Nd contents. The films were deposited directly on SrTiO_3 substrates.

(PCO) and Nd_2CuO_4 (NCO). The a -axis lengths of the three SNCO films deposited on the PCO and the NCO underlayer and a bare STO were 3.946(2), 3.931(2), and 3.918(1) Å, respectively. (The standard deviations of the last significant digit is shown in parentheses.) The a -axis length of an infinite-layer SNCO film deposited on a PCO underlayer was found to be expanded up to a value close to the a -axis length of bulk SNCO.¹

The temperature dependence of electrical resistivity is shown in Fig. 5 for these samples. The films on the PCO underlayer and on a bare STO exhibited superconductivity. The film on the PCO underlayer exhibited a metallic behavior above 100 K. The zero-resistance state was observed below 7 K. However, the film on the NCO underlayer did not show superconductivity. The superconducting properties of SNCO films were very sensitive to the sample preparation conditions. The poor reproducibility in the samples' superconducting property (or electrical resistance) is supposed to be due to defect formation, as often observed in thin film samples of SNCO or infinite-layer $\text{Sr}_{1-x}\text{CuO}_{2-\delta}$.^{10,11} Nevertheless, the thermoelectric-power coefficient is thought to be a good measure to examine electron conduction because thermoelectric power is measured in an open-circuit system and expected to be less sensitive to defects or grain boundaries¹² than electrical resistance or Hall effect.

The temperature dependences of S for these samples are shown in Fig. 6. The values of S were found to be negative throughout the temperature range between 300 and 4.2 K for the films with $x=0.125$ deposited on an NCO underlayer and on a bare STO. On the contrary, those for the film deposited on a PCO underlayer were positive. The value of S increased in the order of cases without underlayer, with an NCO underlayer, and with a PCO underlayer material. It may indicate that the carrier densities in these samples increased in this order. Note that, in the case of $\text{Nd}_{2-x}\text{Ce}_x\text{CuO}_4$ single crystals,¹³ as x increased, the value of S changed from a large negative to a small positive value. Moreover, the S -vs-

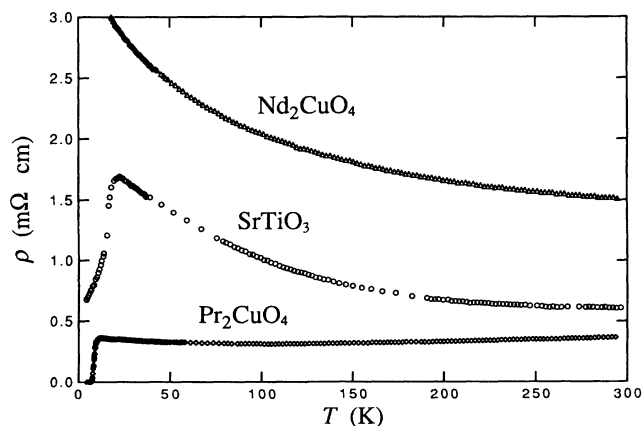


FIG. 5. Temperature dependence of resistivity for the $\text{Sr}_{0.875}\text{Nd}_{0.125}\text{CuO}_{2-\delta}$ thin films deposited on SrTiO_3 substrates with a Pr_2CuO_4 or Nd_2CuO_4 underlayer or without an underlayer. The a -axis lengths of these films were 3.946(2), 3.931(2), and 3.918(1) Å, respectively. The standard deviation of the last significant digit is shown in parentheses.

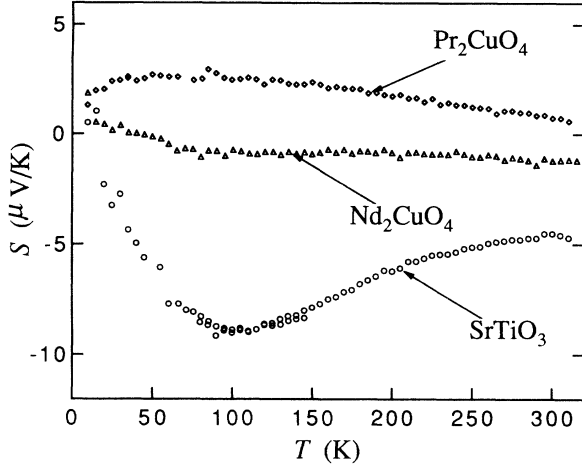


FIG. 6. Temperature dependence of thermoelectric-power coefficient for the $\text{Sr}_{0.875}\text{Nd}_{0.125}\text{CuO}_{2-\delta}$ thin films deposited on SrTiO_3 substrates with a Pr_2CuO_4 or Nd_2CuO_4 underlayer or without an underlayer.

temperature curves look to depend on the underlayer materials, indicating that the electronic structure of SNCO would have been changed as the lattice dimension of underlayer material varied.

SNCO film samples with a low Nd content ($x=0.05$) were fabricated on various underlayer materials: PCO, NCO, and Sm_2CuO_4 (SCO). The SNCO film was also deposited on a bare STO. The a -axis lengths of the SNCO films deposited on PCO, NCO, SCO, and STO were determined to be 3.929(3), 3.933(1), 3.909(3), and 3.907(1) Å, respectively. Compared with the lattice dimension of the bulk SNCO with the same Nd content,¹ the lattice mismatch between the SNCO film and the underlayer material was the smallest for the film deposited

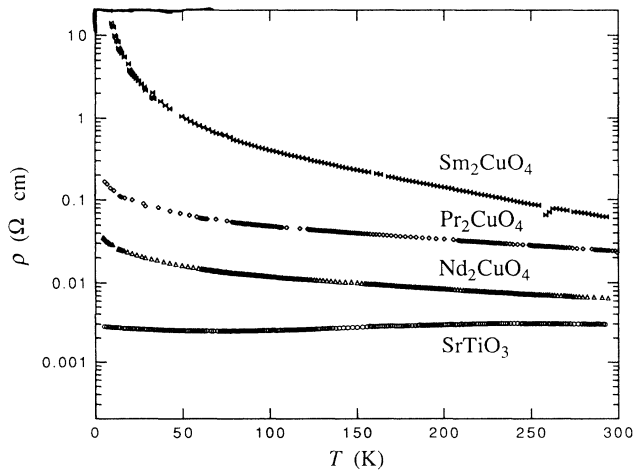


FIG. 7. Temperature dependence of resistivity for the $\text{Sr}_{0.95}\text{Nd}_{0.05}\text{CuO}_{2-\delta}$ thin films deposited on SrTiO_3 substrates with a Pr_2CuO_4 , Nd_2CuO_4 , or Sm_2CuO_4 underlayer or without an underlayer. The a -axis lengths of these films were 3.929(3), 3.933(1), 3.909(3), and 3.907(1) Å, respectively.

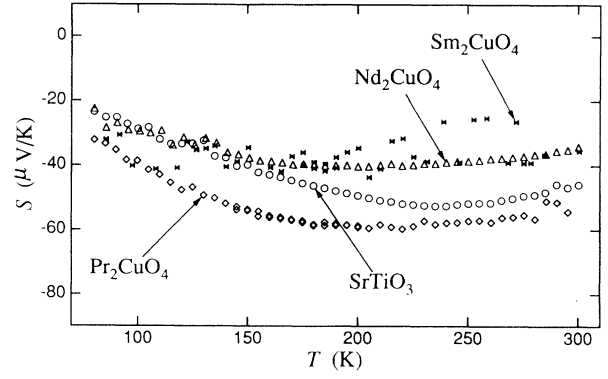


FIG. 8. Temperature dependence of thermoelectric-power coefficient for the $\text{Sr}_{0.95}\text{Nd}_{0.05}\text{CuO}_{2-\delta}$ thin films deposited on SrTiO_3 substrates with a Pr_2CuO_4 , Nd_2CuO_4 , or Sm_2CuO_4 underlayer or without an underlayer.

on NCO. The temperature dependence of electrical resistivity is shown in Fig. 7 for those samples. All the samples exhibit semiconductive behavior. There is no systematic change in the electrical resistivity with respect to the lattice dimension of the underlayer material.

The temperature dependences of S for these films are shown in Fig. 8. All the S -vs-temperature curves were more or less parallel being located within a range as narrow as $\pm 20 \mu\text{V/K}$. The difference of $20 \mu\text{V/K}$ in S corresponds to only a small difference of 0.01 in x (around $x=0.05$) as estimated from the change of S with respect to x given in Fig. 3. This indicates that the differences in the carrier density among the samples were negligibly small.

IV. DISCUSSION

A. Temperature dependence of S

There are several models to explain the nature of S ¹²: the metallic diffusion,¹⁴ the semiconductor band,¹² the variable-range hopping,¹⁴ and the correlated hopping model.¹⁵ Moreover, the contribution from the phonon drag^{16,17} and the magnon drag^{16,17} should be counted. When the data of electrical resistivity are taken into account, the metallic diffusion model is not applicable except for the sample with $x=0.125$ deposited on the PCO underlayer. The semiconductor band model is not applicable either because the absolute value of S should increase with decreasing temperature in this model¹² being contrary to the experimental data. However, this model may be applicable at high temperatures, because the absolute value of S decreases with increasing temperature at high temperatures, e.g., at temperatures higher than 260 K for the $x=0.0$ sample. We employed the variable-range hopping model for the samples with $x=0.0$, 0.05, and 0.075. In this model, resistivity is expected to vary following the relation

$$\ln \rho \propto T^{-\alpha}, \quad (2)$$

where ρ is resistivity and $\alpha = \frac{1}{3}$ ($\frac{1}{4}$) for two-dimensional

(three-dimensional) transport.¹⁴ The thermoelectric-power coefficient is predicted¹⁸ to vary as

$$S \propto \sqrt{T} . \quad (3)$$

The temperature dependence of resistivity can be fitted based on the two-dimensional model only for the sample with $x=0.0$, as shown in Fig. 9. However, it is difficult to identify carriers which dominates electrical conduction in such a system with low carrier density as the sample with $x=0.0$. Figure 10 shows the plots of the absolute values of S for the samples with $x=0.0$ and 0.05 in terms of \sqrt{T} . The curve fitting shown in Fig. 10 is poor. Thus, we concluded that the variable-range hopping model is not applicable.

We consider that the correlated hopping model may be applicable in a high-temperature region where the thermoelectric power is independent of temperature. The formation of a peak in Fig. 3 could be interpreted as a contribution from the magnon drag effect. The shift of the peak along the temperature axis is likely to correspond to the change in the Néel temperature due to electron doping, as was observed in $\text{Nd}_{2-x}\text{Ce}_x\text{CuO}_4$.¹⁹ Phonon drag peaks are usually observed in metallic compounds.¹² Therefore, phonon-drag contributions in the present data would be negligible. The conduction mechanism was considered to be more complicated for the samples with $x=0.10$ and 0.125 because of an anticipated crossover in the conduction mechanism from one due to hopping electrons to another due to itinerant electrons. At present, no perfect models which can explain the behavior of thermoelectric power of the high- T_c superconducting materials are available.

B. Composition dependence of S

The thermoelectric-power coefficients at 300 K for all the samples are plotted in Fig. 7 as a function of the Nd content, x . The correlated hopping mechanism¹⁵ based on the Hubbard model gives S as follows at the high-temperature limit:

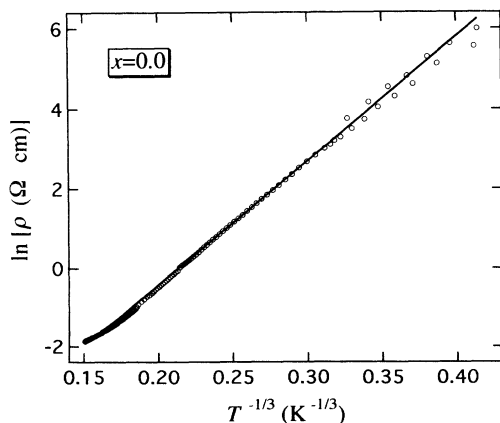


FIG. 9. $\ln \rho$ vs $T^{-1/3}$ being based on the two-dimensional variable-range hopping mechanism for the $\text{SrCuO}_{2-\delta}$ film deposited on SrTiO_3 substrate without an underlayer.

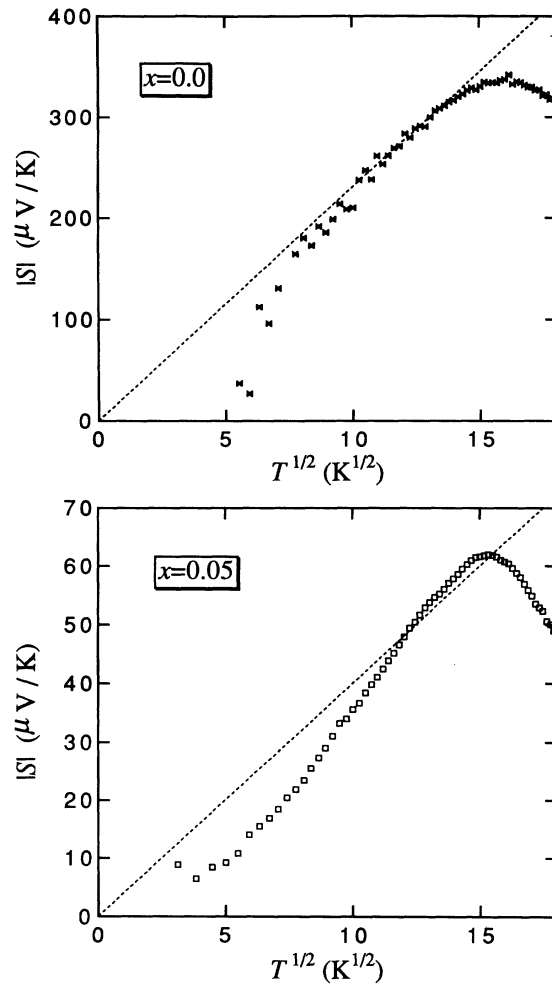


FIG. 10. Plots of the absolute values of S vs square root of temperature for the $\text{Sr}_{1-x}\text{Nd}_x\text{CuO}_{2-\delta}$ films with $x=0.0$ and 0.05 deposited on SrTiO_3 substrates without an underlayer.

$$S = - \frac{k_B}{|e|} \ln \left[\frac{2(1-n)}{n} \right] , \quad (4)$$

where k_B is the Boltzmann constant, e the elementary charge, and n the number of electrons per Cu site. Assuming a relation $n=x$ in Eq. (4), a theoretical curve for S is shown in Fig. 11 by the solid line. Surprisingly, the theoretical curve is quite parallel to the experimental data. The difference between the theoretical and experimental values is nearly independent of temperature being approximately equal to 260 $\mu\text{V/K}$. A similar behavior was observed in the $\text{Nd}_2\text{CuO}_{4-x}\text{F}_x$ system.⁸ The origin of this is not clearly known at present.

C. Effect of Cu-O bond length

Now we discuss the effect of stress caused by the lattice mismatch between the film and the underlayer material on both carrier doping and electron transport. The bond-valence-sum calculation is a useful tool to get information on the valences of constituent ions, the lattice dis-

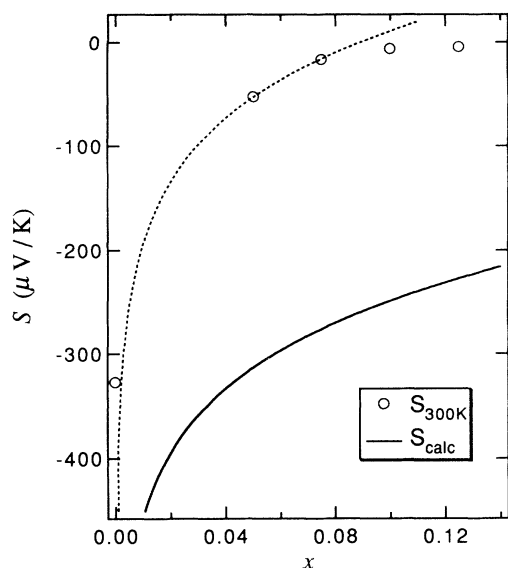


FIG. 11. Relationship between thermoelectric-power coefficient (S) and Nd content, x , for the $\text{Sr}_{1-x}\text{Nd}_x\text{CuO}_{2-\delta}$ films deposited on SrTiO_3 substrates. The open circles represent the measured data at 300 K; the solid line shows a theoretical curve for S on x using Eq. (4) with the assumption of $n = x$; the dashed line is only the guide to the eye.

tortion and the charge transfer between ions in the lattice using experimental crystallographic data.²⁰ The bond-valence-sum may be given as follows according to Brown and Shannon:²¹

$$V_i = \sum_j \exp \left[\frac{R_0 - R_{ij}}{B} \right], \quad (5)$$

where V_i is the bond-valence sum of atom i , R_0 represents the standard bond length between atoms i and j of unit valence, R_{ij} is the measured bond length, and B is a constant equal to 0.37 Å. The value of R_0 used for (Sr, Nd)-O was the mean value weighted with the compositional ratio of Sr and Nd ions of the values of R_0 for Sr-O and Nd-O, i.e., 2.118 and 2.105 Å, respectively. Because R_0 for Cu ion changes with the valence of Cu, the linear interpolation between Cu(I)-O and Cu(II)-O based on the procedure developed by Brown²⁰ was used. We assumed that the oxygen content is 2.0 and the Cu-O sheet has a square planar coordination. The four-circle x-ray-diffraction analysis²² for the SNCO films with $x = 0.125$ deposited on a STO substrate revealed that the oxygen site occupancy was at least 0.97, and that the Cu-O coordination was square planar without an evident buckling and no apical oxygen ions were coordinated.

The calculated bond-valence sums for the SNCO samples are given in Table I. The bond-valence sums of the Cu ion for all the samples were smaller than the formal valences determined from the chemical formula. This indicates a tendency that the square planar Cu-O sheets will be easily doped with electrons. The bond-valence sum for the Cu ion decreases with increasing the Nd con-

TABLE I. Lattice constants (a and c), bond lengths (R), and bond-valence sums (V) for the film samples with various Nd contents (x) deposited on various underlayer materials.

Underlayer material	x	a (Å)	c (Å)	R (Å) Cu-O	R (Å) (Sr,Nd)-O	V Sr,Nd	V Cu
SrTiO_3	0.000	3.903	3.448	1.951	2.604	2.151	1.863
SrTiO_3	0.050	3.907	3.442	1.954	2.603	2.151	1.845
SrTiO_3	0.075	3.910	3.429	1.955	2.600	2.167	1.831
SrTiO_3	0.100	3.912	3.425	1.956	2.599	2.170	1.826
SrTiO_3	0.125	3.918	3.418	1.959	2.600	2.167	1.802
SrTiO_3	0.050	3.907	3.442	1.954	2.603	2.151	1.845
Sm_2CuO_4	0.050	3.909	3.459	1.954	2.610	2.114	1.838
Nd_2CuO_4	0.050	3.933	3.443	1.967	2.614	2.092	1.743
Pr_2CuO_4	0.050	3.929	3.438	1.965	2.610	2.110	1.758
SrTiO_3	0.125	3.918	3.418	1.959	2.600	2.167	1.802
Nd_2CuO_4	0.125	3.931	3.418	1.966	2.605	2.138	1.751
Pr_2CuO_4	0.125	3.946	3.408	1.973	2.607	2.124	1.697

tent. However, the change in the bond-valence sum looks smaller than the value expected from the change in the amount of Nd ions. The change in the bond-valence sum due to Nd substitution may be canceled out by the increase of compressive stress in the lattice.

The bond-valence sum for the Cu ion in the SNCO of the same composition decreases with increasing the a -axis length. It should be noted that the bond-valence sums for ions under internal stresses differ from the actual valences. The present result of thermoelectric-power measurements for the samples with $x = 0.05$ of various a -axis lengths deposited on different underlayer materials indicates that there are little differences in the actual charges estimated from the thermoelectric-power coefficients. It should be noted that there is little possibility for such a self-doping mechanism as was observed in $T'-L_2\text{CuO}_4$ (Ref. 23) to exist in the infinite-layer compounds because there are no interstitial sites in the infinite-layer crystal, furthermore, there is little possibility of having significant amount of oxygen vacancies. In the case which the nominal Nd content is near the solubility limit, the actual Nd content in the matrix crystal could be decreased from the nominal value when the crystal is under compressive stress by the lattice dimensional mismatch, and accordingly the effective valence of Cu ion might be varied. However, there was little difference between the nominal Nd content (0.125) and the value (0.117) estimated from the four-circle x-ray diffractometry for the film sample deposited directly on STO substrate.²² If the actual valence of the Cu ion is not changed much, the difference in thermoelectric-power coefficient for the samples with $x = 0.125$ of various a -axis lengths should be interpreted by the change in electronic structure caused by a change in the Cu-O bond length. Around the composition of $x = 0.125$, the Cu-O bond length sharply affects the state of the crossover in the conduction mechanism from one due to hopping electrons to another due to itinerant electrons.

V. CONCLUSION

We measured the in-plane thermoelectric-power coefficients (S) of *c*-axis-oriented $\text{Sr}_{1-x}\text{Nd}_x\text{CuO}_{2-\delta}$ [$x \leq 0.125$] (SNCO) thin films consisting of a single-phase infinite-layer compound. The signs of S for the SNCO films deposited on SrTiO_3 substrates were negative and the magnitude of S increased with increasing the Nd content. The temperature dependence of S could not be perfectly explained by any available models. The *a*-axis length of the SNCO film with the same Nd content was dependent on the underlayer material. The value of S for the SNCO film with $x = 0.125$ strongly depended on the

a-axis length, but, that for the SNCO film with $x = 0.05$ was weakly dependent on the *a*-axis length. This strong *a*-axis dependence of the SNCO film with $x = 0.125$ indicates that the conduction mechanism may be drastically changed by a change in the Cu-O bond length in the vicinity of this composition.

ACKNOWLEDGMENTS

The authors wish to express their thanks to Koichi Kubo for his helpful discussion. This work was supported by New Energy and Industry Technology Development Organization for the Research and Development of Industrial Science and Technology Frontier Program.

-
- ¹M. G. Smith, A. Manthiram, J. Zhou, J. B. Goodenough, and J. T. Markert, *Nature* **351**, 549 (1991).
²G. Er, Y. Miyamoto, F. Kanamaru, and S. Kikkawa, *Physica C* **181**, 206 (1991).
³H. Adachi, T. Satoh, Y. Ichikawa, K. Setsune, and K. Wasa, *Physica C* **196**, 14 (1992).
⁴N. Sugii, K. Kubo, M. Ichikawa, K. Yamamoto, H. Yamauchi, and S. Tanaka, *Jpn. J. Appl. Phys.* **31**, L1024 (1992).
⁵C. Niu and C. M. Lieber, *Appl. Phys. Lett.* **61**, 1712 (1992).
⁶N. Sugii, K. Matsuura, K. Kubo, K. Yamamoto, M. Ichikawa, and H. Yamauchi, *J. Appl. Phys.* **74**, 4047 (1993).
⁷See, e.g., D. K. C. MacDonald, *Thermoelectricity* (Wiley, New York, 1962).
⁸J. Sugiyama, K. Matsuura, M. Kosuge, H. Yamauchi, and S. Tanaka, *Phys. Rev. B* **45**, 9951 (1992).
⁹D. P. Norton, B. C. Chakoumakos, E. C. Jones, D. K. Christen, and D. H. Lowndes, *Physica C* **217**, 146 (1993).
¹⁰S. Takeno, S. Nakamura, Y. Terashima, and T. Miura, *Physica C* **206**, 75 (1993).
¹¹N. Sugii, M. Ichikawa, K. Hayashi, K. Kubo, K. Yamamoto, and H. Yamauchi, *Physica C* **213**, 345 (1993).
¹²A. B. Kaiser and C. Uher, in *Studies of High Temperature Superconductors*, edited by A. V. Narlikar (Nova Science, New York, 1990), Vol. 7, pp. 1–40.
¹³X.-Q. Xu, S. J. Hagen, W. Jiang, J. L. Peng, Z. Y. Li, and R. L. Greene, *Phys. Rev. B* **45**, 7356 (1992).
¹⁴See, e.g., N. F. Mott and E. A. Davis, *Electronic Processes in Non-Crystalline Materials*, 2nd. ed. (Clarendon, Oxford, 1979).
¹⁵P. M. Chaikin and G. Beni, *Phys. Rev. B* **13**, 647 (1976).
¹⁶M. Bailyn, *Phys. Rev.* **126**, 2040 (1962).
¹⁷B. Coqblin, *The Electronic Structures of Rare-Earth Metals and Alloys: The Magnetic Heavy Rare-Earths* (Academic, London, 1977), pp. 605–611.
¹⁸I. P. Zvyagin, *Phys. Status Solidi B* **58**, 443 (1973).
¹⁹G. M. Luke, B. J. Sternlieb, Y. J. Uemura, J. H. Brewer, R. Kadano, R. F. Kiefl, S. R. Kreitzman, T. M. Riseman, J. Gopalakrishnan, A. W. Sleight, M. A. Subramanian, S. Uchida, H. Takagi, and Y. Tokura, *Nature* **338**, 49 (1989).
²⁰I. D. Brown, *J. Solid State Chem.* **90**, 155 (1991).
²¹I. D. Brown and R. D. Shannon, *Acta. Crystallogr. A* **29**, 266 (1973).
²²N. Sugii, H. Yamauchi, and M. Izumi, *Phys. Rev. B* **50**, 9503 (1994).
²³J. S. Zhou, J. Chan, and J. B. Goodenough, *Phys. Rev. B* **47**, 5477 (1993).